

RSC Advances



This is an *Accepted Manuscript*, which has been through the Royal Society of Chemistry peer review process and has been accepted for publication.

Accepted Manuscripts are published online shortly after acceptance, before technical editing, formatting and proof reading. Using this free service, authors can make their results available to the community, in citable form, before we publish the edited article. This *Accepted Manuscript* will be replaced by the edited, formatted and paginated article as soon as this is available.

You can find more information about *Accepted Manuscripts* in the [Information for Authors](#).

Please note that technical editing may introduce minor changes to the text and/or graphics, which may alter content. The journal's standard [Terms & Conditions](#) and the [Ethical guidelines](#) still apply. In no event shall the Royal Society of Chemistry be held responsible for any errors or omissions in this *Accepted Manuscript* or any consequences arising from the use of any information it contains.

COMMUNICATION

Delineating *Monascus* azaphilone pigment biosynthesis: oxidoreductive modifications determine the ring cyclization pattern in azaphilone biosynthesis

Cite this: DOI: 10.1039/x0xx00000x

Received 00th January 2012,
Accepted 00th January 2012

DOI: 10.1039/x0xx00000x

Balakrishnan Bijinu,^a Jae-Won Suh,^a Si-Hyung Park,^b and Hyung-Jin Kwon*^a

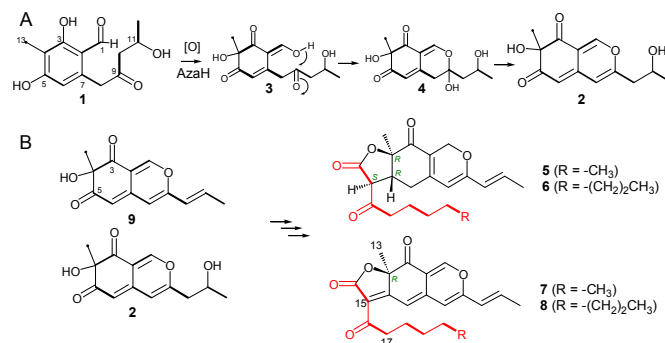
www.rsc.org/

The product profiles of *mppF*, *mppA*, and *mppC* mutants substantiate that MppA-mediated ω -2 ketoreduction is a prerequisite for the synthesis of the pyranoquinone bicyclic core of the *Monascus* azaphilone pigment and that MppC activity determines the regioselectivity of the spontaneous Knoevenagel condensation.

Fungal polyketide synthases (fPKSs) are iteratively acting multi-domain polypeptides and generally classified as non-reducing- (NR-), partially reducing-, or highly reducing-types, depending on the extent of reductive modifications that occur during the assembly of acetate units through a decarboxylative Claisen condensation.¹ Azaphiloid is a class of polyketides that bears a highly oxygenated pyranoquinone bicyclic core and is generally known of fungal origin.² The azaphilone polyketide is synthesized by an NR-fPKS with a reductive release domain (-R), and the pyran ring cyclization follows a hydroxylation-mediated dearomatization of a benzaldehyde intermediate, as shown in azanigerone biosynthesis (Scheme 1A).³ Azanigerone NR-fPKS-R incorporates one acetyl-CoA, five malonyl-CoAs, and a methyl moiety from *S*-adenosyl methionine; the resulting polyketide intermediate undergoes a ketoreduction at the C-11 position, generating FK17-P2a (**1**), but the timing of this ketoreduction is unresolved. A biochemical study clearly demonstrated that a monooxygenase AzaH introduces a hydroxyl group at the C-4 position of **1** to generate azanigerone E (**2**) (Scheme 1A).⁵ This conversion was proposed to involve **3** and **4**. We maintain the position numbering pattern used in the structures of **1** and **2** throughout this report in order to emphasize the biosynthetic relatedness of the compounds described.

Monascus species including *M. pilosus*, *M. purpureus*, and *M. ruber* are known to produce *Monascus* azaphilone pigments (MAZPs), which are the active ingredients of the traditional food colorant derived from the fermentation of *Monascus*.⁴ It is also known that some MAZPs display diverse biological activities that include anti-diabetic, anti-inflammatory, anti-atherosclerotic, and anti-cancer activities.⁵⁻⁸ MAZPs include ankaflavin (**5**), monascin (**6**), rubropunctatin (**7**), and monascorubrin (**8**) (Scheme 1B). The MAZP biosynthetic gene cluster was previously described, and a genetic knockout of the MAZP PKS gene (*MpPKS5*) abolished MAZP production in *M. purpureus*.⁹ *MpPKS5* belongs to NR-fPKS-

R. *MpFAS2*, the canonical fatty acid synthase encoded in the gene cluster, was also shown to be essential for MAZP biosynthesis.¹⁰ *MpFAS2* is proposed to synthesize short-chain 3-oxo-fatty acyl thioesters for MAZP biosynthesis. The MAZP biosynthetic gene cluster encodes an acyltransferase MppB, which is assigned as the catalyst that mediates the installation of the *MpFAS2* products at the tertiary alcoholic oxygen at C-4 (Scheme 1B).



Scheme 1 (A) AzaH-mediated pyran ring cyclization mechanism. (B) The proposed biosynthetic origin of MAZP with the role of the acyltransferase MppB and the MAZP fatty acid synthase *MpFAS2*. Bold lines and black circles denote acetate units and *S*-adenosyl methionine-derived carbons.

We also confirmed that the *mppB*-knockout mutant is incapable of producing MAZP (data not shown). Knoevenagel condensation between the α carbon of the 3-oxo-fatty moiety and the C-5 carbonyl group may generate a 2-furanone moiety, leading to the production of **5-8** (Scheme 1B). The biosynthetic study of chaetoviridin in *Chaetomium globosum* demonstrated that the 2-furanone-forming cyclization is non-enzymatic,¹¹ but the nature of this reaction for **5-8** is yet to be unveiled because the ring cyclization geometry for **5-8** differs from that for chaetoviridin. The pyranoquinone bicyclic structure of **7** and **8** is identical to **2**, but the exocyclic 2-hydroxypropane moiety of **2** is replaced with a propene moiety in **7** and **8**. This suggests two plausible scenarios for *MpPKS5* catalysis: crotonyl-CoA serves as the starting unit to

generate **9** or MpPKS5 generates **2** through the same synthetic route as azanigerone (Scheme 1B). The latter scenario requires a dehydration step to yield MAZP. With the presumed intermediacy of **2** or **9** in MAZP biosynthesis, it has been tempting to think of **7/8** as the precursor to **5/6**. It was previously shown that an *mpp7* knockout resulted in accumulation of monasfluor A (**10**) and B (**11**) without **5-8** (Scheme 2).¹² Mpp7 was proposed to control the regioselectivity of the Knoevenagel aldol condensation. Although the catalytic role of Mpp7 was not defined, accumulation of **10** and **11** supports the idea that **2** is the true intermediate of MAZP biosynthesis. In order to assess the polyketide intermediate of MAZP biosynthesis, the homolog of *azaH* (*mppF*) was inactivated in the MAZP biosynthetic gene cluster (see ESI† for gene inactivation), which resulted in a high accumulation of **1** (Figure 1B; see ESI† for NMR spectra). In this report, the LC-MS result of the culture supernatant extract is provided (see ESI† for LC-MS result of the culture mycelium extract).

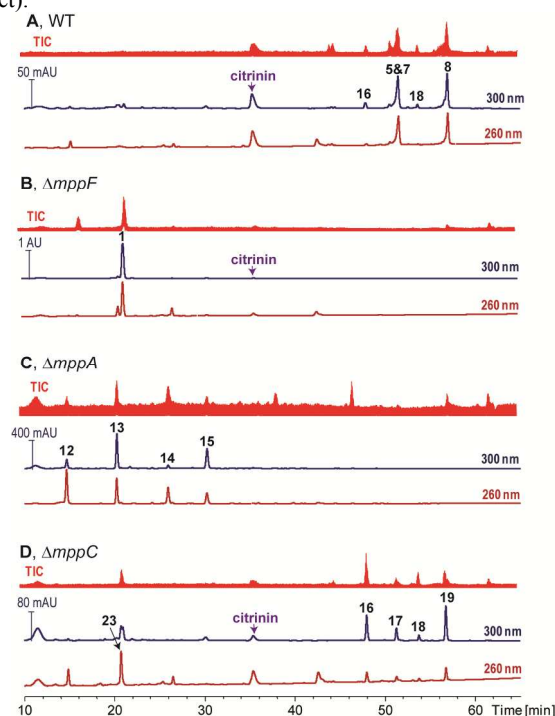
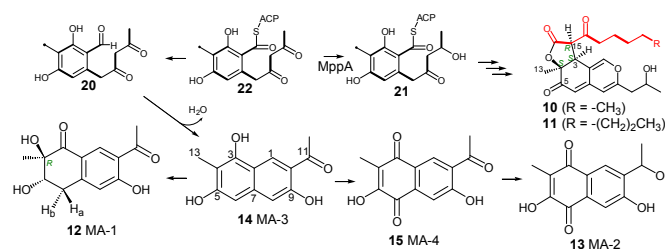


Fig. 1 LC-MS analysis of the culture supernatant extracts of *M. purpureus* WT (A) and the mutants of *mppF* (B), *mppA* (C), and *mppC* (D).

Administration of **1** to the MpPKS5 knockout mutant restored the production of **5-8** (data not shown). This experiment established that the early biosynthetic route of MAZP is common to that of azanigerone. In the azanigerone biosynthetic gene cluster, two oxidoreductase genes *azaE* and *azaJ* were identified.³ AzaE was proposed to mediate the ketoreduction that is required for the generation of **1**, but there is no experimental data supporting this functional assignment. The MAZP biosynthetic gene cluster encodes three reductase candidates, MppA, MppC, and MppE, but none of them bears a significant homology with AzaE. Instead, AzaJ has a significant homology with MppE (47% identity/62% similarity). To access the roles of the oxidoreductive modifications in the MAZP biosynthesis, we generated genetic knock-out mutants of *mppA* and *mppC* in *M. purpureus* (see ESI† for gene inactivation). Inactivation of *mppE* could not be achieved for unidentified reasons; the role of MppE in the MAZP biosynthesis is yet to be unveiled. An *mppC*-knockout mutant of *Monascus ruber* was reported to accumulate yellow pigments other than **5-8**.¹³ However, the identities of these

pigments were not determined. LC-MS analysis indicated that MAZPs are below the detection level in the *mppA* mutant. Instead, this mutant accumulated four compounds (**12-15**), which eluted substantially faster than **5-8** (Figure 1C). MS analysis identified the molecular ions of $[M+H]^+$ 251, 249, 233, and 247, for **12**, **13**, **14**, and **15**, respectively, substantiating that **12-15** were devoid of the short fatty acyl chain. The *mppC* mutant produced four compounds, which possessed elution times similar to those of **5-8** (Figure 1D). These yellow pigments have molecular masses comparable to those of **5-8**, with molecular ion peaks of $[M+H]^+$ at m/z 357, 355, 385, and 383 (**16** to **19**), respectively.



Scheme 2 Structure of **12-15** and the proposed biosynthetic route highlighting the catalytic role of MppA.

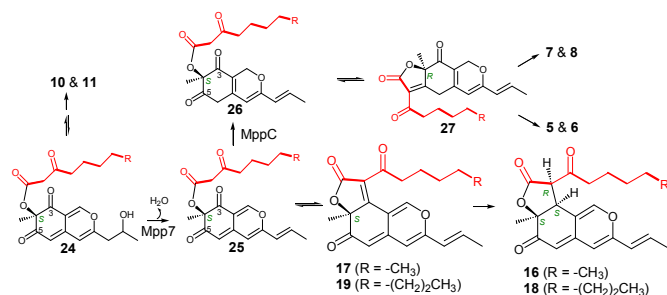
We purified **12-15**, which have the names of MA-1 to -4 in our lab, respectively, and determined their structures (Scheme 2; see ESI† for structural determination). **12** and **14** appear structurally related. It is thus tempting to suggest that **14** is converted into **12** by the MppF-mediated hydroxylation and then subsequent reduction. **12** is the previously reported 1-tetralone compound (monaspurpurone) from *M. purpureus*.¹⁴ Although the monaspurpurone isolate was found to be racemic,¹⁴ we assume here that the C-4 of **12** retains the same *R*-configuration as **5-8**. **14** has not previously been identified to the best of our knowledge. **13** and **15** were 1,4-naphthoquinone derivatives known to be produced by a *A. nidulans* transformant of an NR-fPKS-R gene (ATEG_03432) of *A. terreus* origin.¹⁵

The notable structural feature of **12-15** is their C10 bicyclic core, suggesting that they are generated by a Knoevenagel aldol condensation of the presumed intermediate, **20**. It seems plausible that MppA is involved in the formation of **21** (Scheme 2). The timing of the MppA-mediated ketoreduction, whether it occurs on the very early intermediate (acetoacetyl-thioester tethered on the acyl carrier domain) or it precedes the reductive release from MpPKS5, could not be determined. We here adopt the latter scenario due to the considerable yield of **12-15**: their isolation yields from a 1.5 liter culture were 37, 14, 29, and 8 mg, respectively. In the former scenario, acetoacetyl-thioester tethered on MpPKS5 will be generated in the *mppA* mutant. MpPKS5 is probably incapable of processing efficiently this aberrant intermediate, giving rise to a low level of **12-15**, even if they are produced. The biosynthetic proposal for **12-15** is that **22** is released from MpPKS5, and the resulting compound **20** is converted into the C10 bicyclic structure. We also propose that the MppA-mediated ketoreduction suppresses the spontaneous Knoevenagel aldol condensation that leads to **12-15** by lowering acidity of the C-10 position, paving the way to a pyranoquinone bicyclic structure.

MppA is 297 amino acids long and belongs to the Rossmann-fold NAD(P)⁺-binding protein family (cd05233, COG1028). In terms of polyketide biosynthesis, MppA can be classified as a member of the ketoreductase family. MppA is homologous to *A. terreus* ATEG_03438 (59% identity/77% similarity) and *mppA* is neighbored by the aforementioned NR-fPKS-R gene, ATEG_03432 that generated **13** and **15** in an ectopic expression.¹⁵ The *azaH* (the

C-4 hydroxylase gene) homolog (*ATEG_03443*) can also be found nearby *ATEG_03432*. It is thus tempting to suggest that the gene cluster containing *ATEG_03432* encodes the biosynthesis of a yet-unknown azaphilone compound. The azanigerone gene cluster does not harbor an *mppA* homolog, while **2** is predicted to be the common intermediate in both of the azanigerone and MAZP pathways. There are two possibilities. One is that MppA and its counterpart in the azanigerone pathway are not similar due to their convergent evolution. The other is that the timing of this ketoreduction differs in two pathways, and thus, the two ketoreductases differ intrinsically.

The four compounds in the *mppC* mutant are identified as MAZP derivatives (**16-19**, named MC-1 to -4 in our experiments), possessing the lactone (2-furanone for **17** and **19**) ring geometry of **10** and **11** (Scheme 3).¹² LC-MS analysis indicated that small amounts of **16** and **18** were also detectable in WT (Figure 1A). It was thus possible that trace amounts of **17** and **19** also existed in the WT extract, but this LC-MS analysis could not identify them due to their overlapping with **7** and **8** in the elution. The structural determination of **16-19** was straightforward due to their resemblance to **10** and **11** (see ESI† for NMR spectra). **16** and **18** are notably different from **10** and **11** in possessing two allylic proton signals at δ_{H} (ppm) 6.54 (10-*H*, doublet of quartet) and 5.99 (11-*H*, doublet). **16** and **18** were found to be identical to monasfluore A and B, respectively, which were reported from a *Monascus* species (Scheme 3).¹⁶ **17** and **19** are novel MAZP derivatives possessing a double bond between C-3 and C-15 (Scheme 3). A reduction may convert **17** and **19** into **16** and **18**, respectively, but the reduction catalyst is unknown, as in the case for **10** and **11**.¹² In the *mppC* mutant, another compound (**23**) was accumulated (Figure 1D). The elution time of **23** was similar to those of **1** and **13**, but the mass analysis (m/z 237 and 259 for $[\text{M}+\text{H}]^+$ and $[\text{M}+\text{Na}]^+$, respectively) indicated that **23** is distinct from them. We completed structural determination of **23** (see ESI† for NMR spectra and the structure), identifying it as FK17-P2b1, which was previously reported from *Aspergillus* sp.¹⁷ and later from a yellow mutant of *Monascus kaoliang*.¹⁸ **23** is closely related to monascusone A¹⁸ that was previously found to accumulate in the *MpfasB* mutant.¹⁰



Scheme 3 Structure of **16-19** and the proposed biosynthetic route featuring the role of MppC controlling the regioselectivity of the intramolecular Knoevenagel condensation. R is $-\text{CH}_3$ or $-(\text{CH}_2)_2\text{CH}_3$ in the cases of **24-27**.

Accumulation of **10** and **11** in the *mpp7* mutant had previously led us to propose that Mpp7 controls regioselective Knoevenagel condensation during the 2-furanone ring formation.¹² The ring cyclization geometry for **10** and **11** is the same as that for chaetoviridin.¹¹ It was thus proposed that the ring cyclization for **5-8** demands Mpp7, while the reaction for **10** and **11** is non-enzymatic as shown in chaetoviridin biosynthesis.^{11,12} The biochemical role of Mpp7 was veiled because it bears no significant sequence homology to other proteins with known biochemical functions. However, it was found that the *mppC* mutant (*mpp7⁺/mppC*) accumulated **16-19** that

have the ring geometry of **10** and **11** (Figure 1D). This result indicates that Mpp7 alone is incapable of completing the regioselective Knoevenagel condensation for **5-8**. It seems more likely that an Mpp7-mediated modification is a factor affecting the regioselectivity of the aldol condensation. The intermediacy of **1** (Figure 1A) strongly supports the involvement of a dehydration step in MAZP biosynthesis. We here propose that Mpp7 is the dehydratase. In the proposed biosynthetic pathway, **2** is acylated by MppB into **24**, which is then converted into **25** by Mpp7 (Scheme 3). In the absence of Mpp7, **24** is converted to **10/11** through a Knoevenagel aldol condensation/cyclization and then subsequent reduction. The reduction step is efficient enough to drive the quantitative conversion of **24** into **10/11**: the *mpp7* mutant yielded a large accumulation of **10** and **11** with no other notable pigment product.¹² In the case of **17/19**, the reductive conversion into **16/18** is relatively inefficient, allowing a comparable balance between **17/19** and **25**. This situation resulted in the hydrolysis of **25** into **9**, which is then converted into **23** (see ESI† for proposed biosynthetic route of **23**). As demonstrated in the chaetoviridin biosynthesis,¹¹ together with the occurrence in **10-11** and **16-19**, the nucleophilic attack of C-15 occurs to C-3 carbonyl but not to C-5, as for **24** and **25**. This regioselectivity may operate because C-3 is a better electron acceptor than C-5, which belongs to an extended π -conjugated system of the 4*H*-pyran-4-ylidene moiety. It is thus reasonable to envision that MppC induces a structural change in the pyranoquinone structure of **25**. We propose here that MppC reduces **25** into **26**, making C-5 a better electron acceptor by eliminating the π -conjugated system of **25** (Scheme 3). In this proposal, the resulting compound **27** undergoes two parallel reactions each of which leads to **5/6** and **7/8**.

Conclusions

The present study advances our understanding of the chemical strategy used in the azaphilone biosynthesis. This study defines NR-IPKS-R, MppA, and MppF as a catalytic tool-kit for azaphilone biogenesis. The study of MppC provides a lesson on how the divergence of the azaphilone pathway evolved: the coordination of oxidoreductive catalyst in altering the geometric specificity of the spontaneous Knoevenagel aldol condensation.

Notes and references

^a Department of Biological Science, Myongji University, Yongin 449-728, Republic of Korea. E-mail: hjink@mju.ac.kr.

^b Department of Oriental Medicine Resources, Mokpo National University, Muan 534-729, Republic of Korea.

* This research was supported by Basic Science Research Program through the National Research Foundation of Korea (NRF) funded by the Ministry of Education (2013R1A1A2059458).

† Electronic Supplementary Information (ESI) available: Experimental details, extra liquid chromatograms, NMR spectra, and UV-Vis absorption spectra. See DOI: 10.1039/c000000x/

- R. J. Cox, *Org. Biomol. Chem.*, 2007, **5**, 2010-2026.
- J. M. Gao, S. X. Yang and J. C. Qin, *Chem. Rev.*, 2013, **113**, 4755-4811.
- A. O. Zabala, W. Xu, Y. H. Chooi and Y. Tang, *Chem. Biol.*, 2012, **19**, 1049-1059.
- Y. Feng, Y. Shao and F. Chen, *Appl. Microbiol. Biotechnol.*, 2012, **96**, 1421-1440.
- L. C. Hsu, Y. W. Hsu, Y. H. Liang, C. C. Liaw, Y. H. Kuo and T. M. Pan, *Molecules*, 2012, **17**, 664-673.
- C. L. Lee, Y. P. Hung, Y. W. Hsu and T. M. Pan, *J. Agric. Food Chem.*, 2013, **61**, 143-150.
- C. L. Lee, J. Y. Wen, Y. W. Hsu and T. M. Pan, *J. Agric. Food Chem.*, 2013, **61**, 1493-1500.

8. L. C. Hsu, Y. H. Liang, Y. W. Hsu, Y. H. Kuo and T. M. Pan, *J. Agric. Food Chem.*, 2013, **61**, 2796-2802.
9. B. Balakrishnan, S. Karki, S. H. Chiu, H. J. Kim, J. W. Suh, B. Nam, Y. M. Yoon, C. C. Chen and H. J. Kwon, *Appl. Microbiol. Biotechnol.*, 2013, **97**, 6337-6345.
10. B. Balakrishnan, H. J. Kim, J. W. Suh, C. C. Chen, K. H. Liu, S. H. Park and H. J. Kwon, *J. Korean Soc. Appl. Biol. Chem.*, 2014, **57**, 191-196.
11. J. M. Winter, M. Sato, S. Sugimoto, G. Chiou, N. K. Garg, Y. Tang and K. Watanabe, *J. Am. Chem. Soc.*, 2012, **134**, 17900-17903.
12. B. Balakrishnan, C. C. Chen, T. M. Pan and H. J. Kwon, *Tetrahedron Lett.*, 2014, **55**, 1640-1643.
13. Q. Liu, N. Xie, Y. He, L. Wang, Y. Shao, H. Zhao and F. Chen, *Appl. Microbiol. Biotechnol.*, 2014, **98**, 285-296.
14. M. J. Cheng, M. D. Wu, I. S. Chen, C. Y. Chen, W. L. Lo and G. F. Yuan, *Nat. Prod. Res.*, 2010, **24**, 1719-1725.
15. Y. M. Chiang, C. E. Oakley, M. Ahuja, R. Entwistle, A. Schultz, S. L. Chang, C. T. Sung, C. C. Wang and B. R. Oakley, *J. Am. Chem. Soc.*, 2013, **135**, 7720-7731.
16. Z. Huang, Y. Xu, L. Li and Y. Li, *J. Agric. Food. Chem.*, 2007, **56**, 112-118.
17. T. Arai and H. Sano, Patent No. J.P. 6,329,576, 1997, November 29.
18. S. Jongrungruangchok, P. Kittakoop, B. Yongsmith, R. Bavovada, S. Tanasupawat, N. Lartpormmatulee and Y. Thebtaranonth, *Phytochemistry*, 2004, **65**, 2569-2575.

Coordination of oxidoreductive modifications in controlling ring cyclization pattern in azaphilone biosynthesis